FIG. 1 Aggregate Particle Size Response of Control and Biotinylated Perfluorocarbon Emulsions to Titrated Levels of Avidin

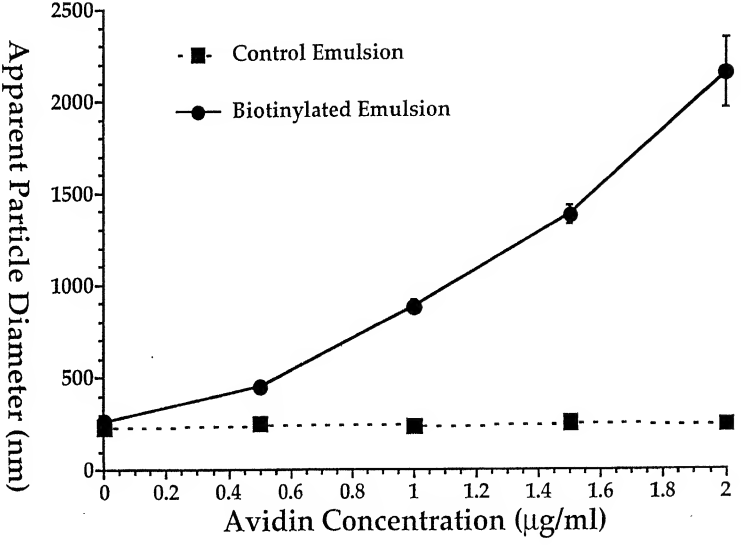

FIG. 2 ULTRASONIC IMAGES OF CONTROL AND BIOTINYLATED PERFLUOROCARBON EMULSION BEFORE AND AFTER THE ADDITION OF AVIDIN

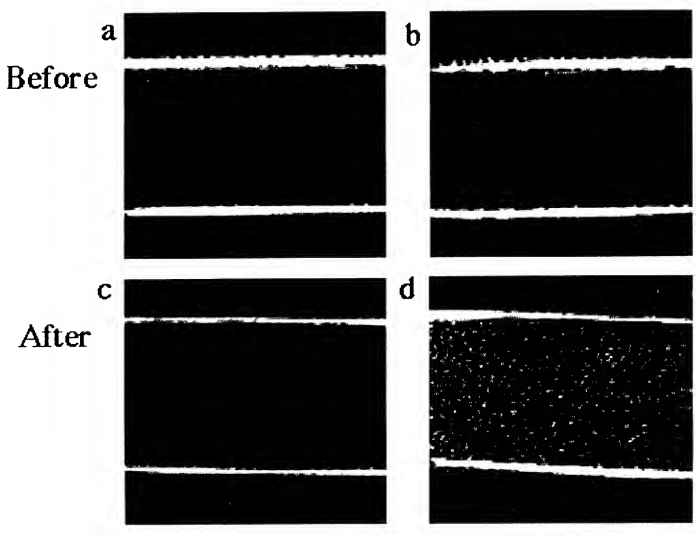

Figure 3. Graphic Illustration of Dialysis Tubing Images and Region of Interest Placement for Gray Scale Analysis

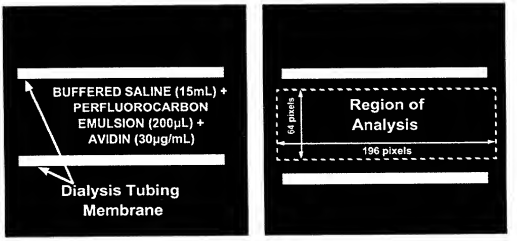

FIG.4 Changes in Average Pixel Gray Scale Associated with the Addition of Avidin to Control or Biotinylated Perfluorocarbon Emulsion

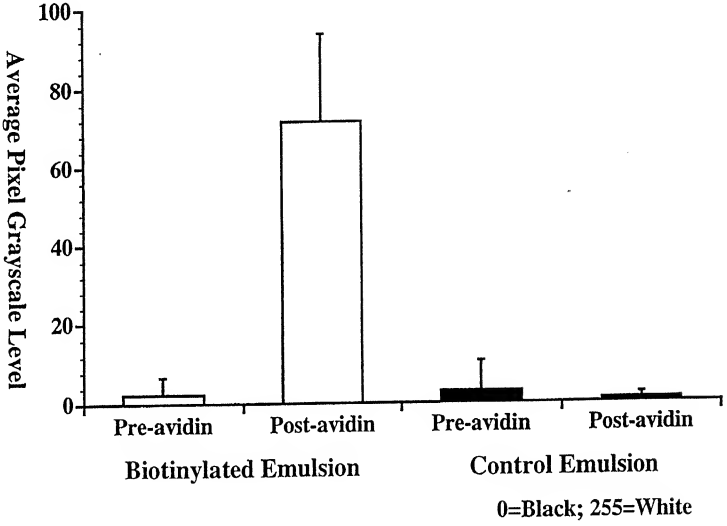

FIG.5 The Effect of Control and Biotinylated Perfluorocarbon Emulsion on Apparent Backscatter Transfer Function and Integrated Backscatter of Avidinized Nitrocellulose Membranes

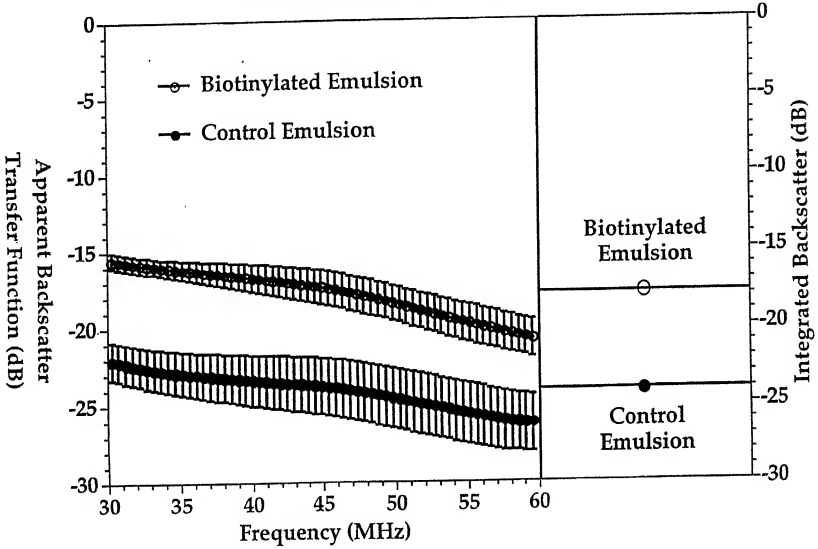

5/21

FIG.6 **Apparent Backscatter Transfer Function of Biotinylated and Control Perfluorocarbon Emulsions Targeted to D-dimer Covalently Conjugated to Nitrocellulose Membranes**

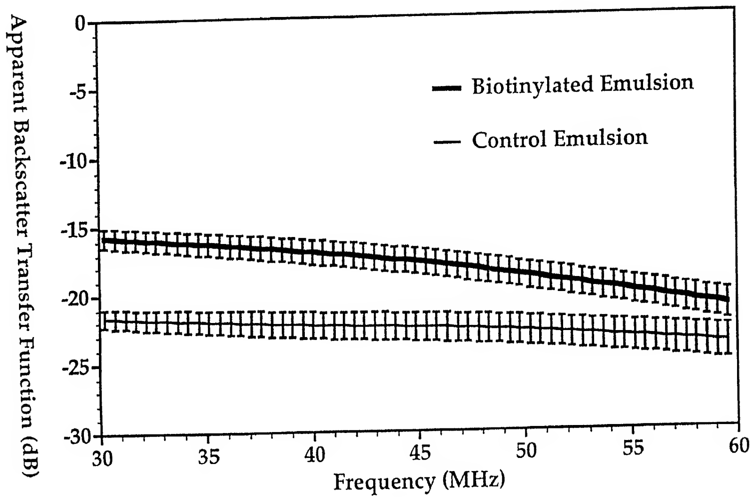

FIG.7 Apparent Backscatter Transfer Function (dB) of Biotinylated and Control Perfluorocarbon Emulsions at Low Ultrasonic Frequencies

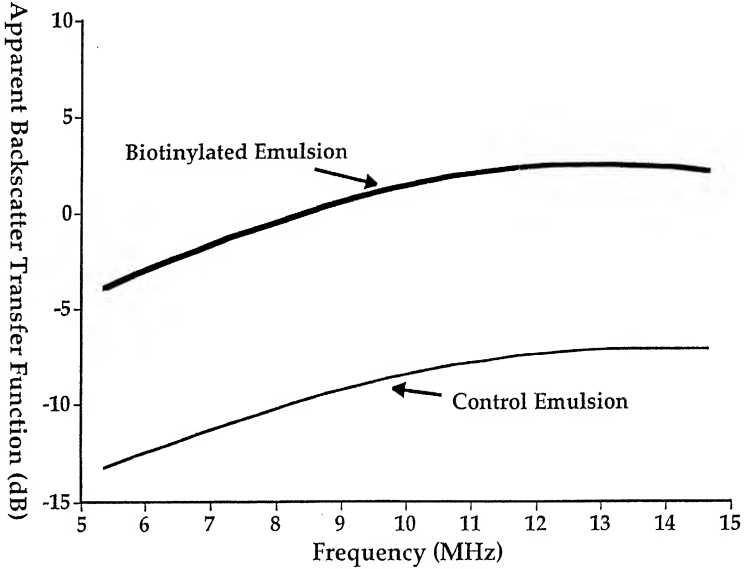

FIG.8 Apparent Backscatter Transfer Function of Biotinylated and Control Perfluorocarbon Large Particle Size Emulsions Targeted to Avidinized Nitrocellulose Membranes

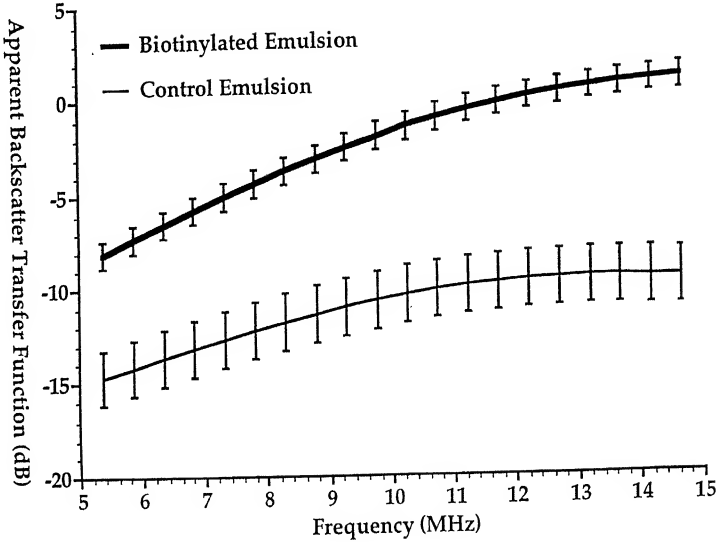

Figure 9. Ultrasonic Images (7.5 MHz) of Plasma Thrombi Pre-targeted with Antifibrin Monoclonal Antibody and Exposed to Control or Biotinylated Perfluorocarbon Emulsion *in Vitro*

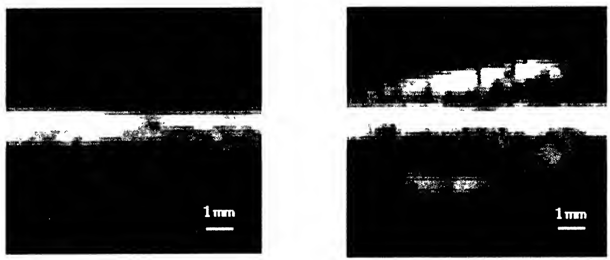

Control Emulsion   Biotinylated Emulsion

FIG. 10 Average Pixel Grayscale of Plasma Thrombi Pre-targeted with Antifibrin Monoclonal Antibody and Exposed to Control or Biotinylated Perfluorocarbon Emulsion

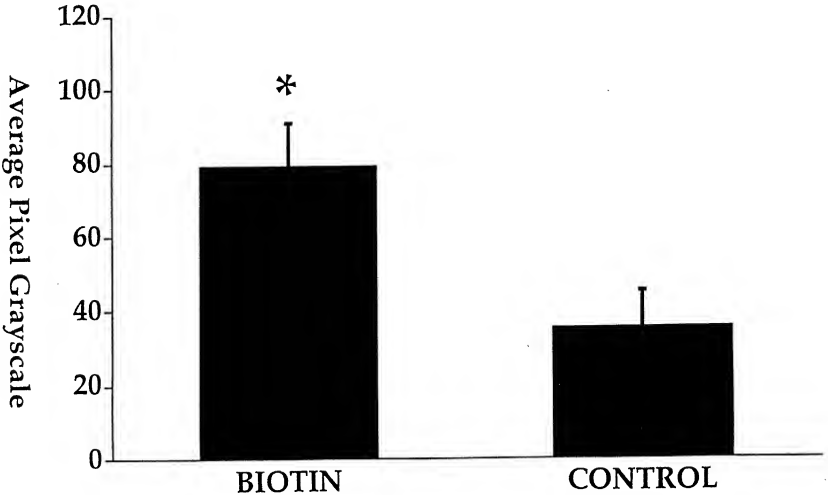

Figure 11. Femoral Artery Thrombus Acoustically Enhanced with Biotinylated Perfluorocarbon Emulsion *In Vivo*

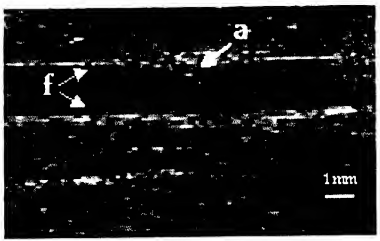

Thrombus Before Targeted Biotinylated Contrast

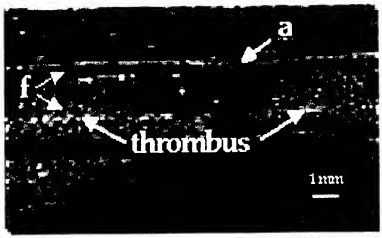

Thrombus After Targeted Biotinylated Contrast

Imaged with HP Sonos 2500
7.5 MHz Focused, Linear Phased Array Transducer

Key: a=electrical anode; f=femoral artery walls

FIG.12 Net Change in Apparent Backscatter Transfer Function of Biotinylated and Control Perfluorocarbon Emulsions Targeted to Prostate Specific Antigen in Prostatic Carcinoma Relative to Normal Regions

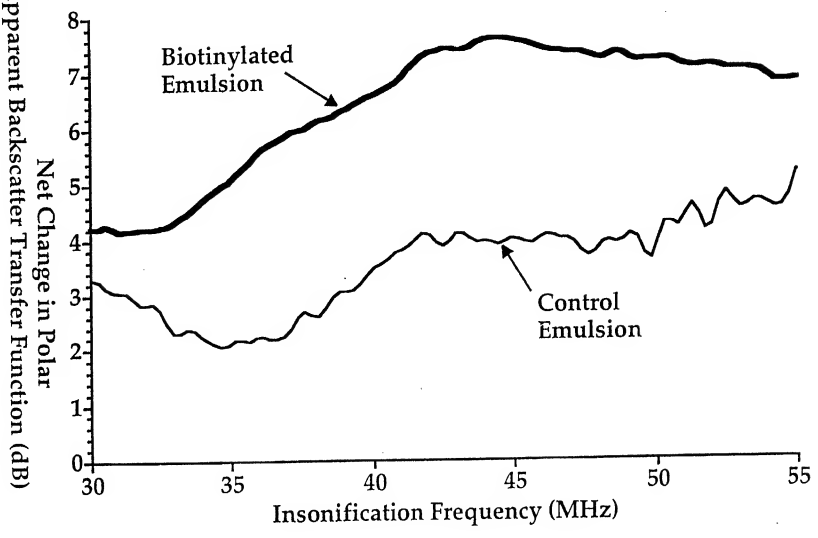

FIG. 13 Net Change in Integrated Backscatter between Normal Prostatic Stroma and Cancer Regions for Control versus Biotinylated Perfluorocarbon Emulsions

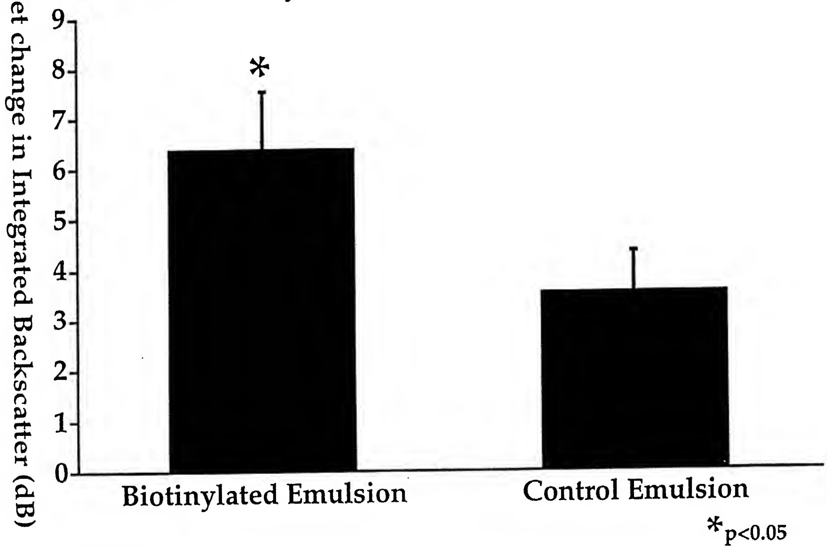

FIG. 14 Net Change in Apparent Backscatter Transfer Function of Biotinylated and Control Perfluorocarbon Emulsions Targeted to OC-125 Antigen in Ovarian Carcinoma Relative to Normal Regions

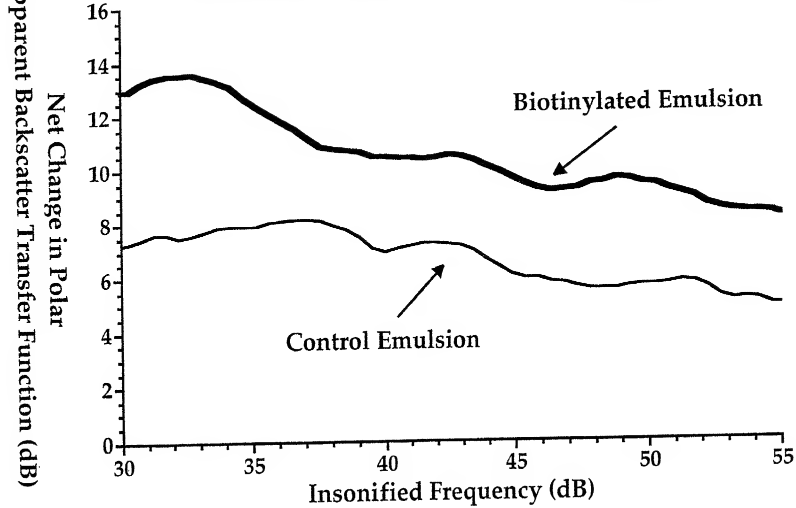

FIG. 15 Net Change in Integrated Backscatter Between Normal Ovarian Tissue and Carcinoma Regions for Control versus Biotinylated Perfluorocarbon Emulsions

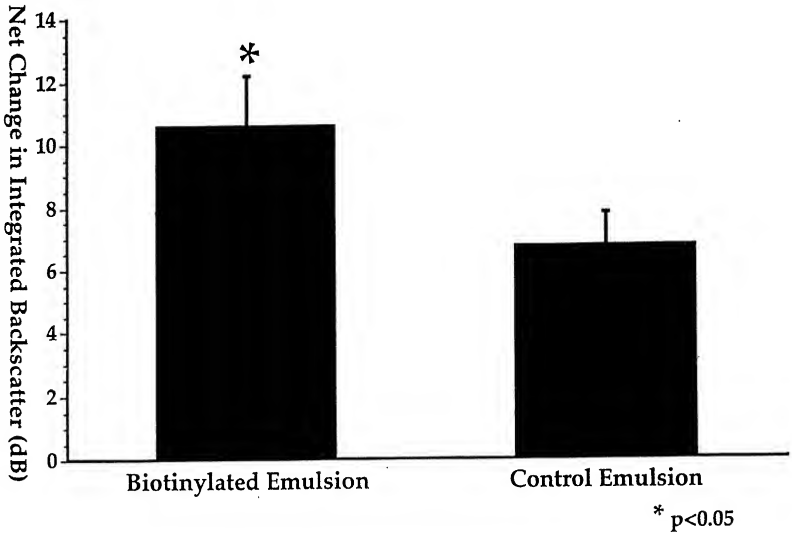

Figure 16. Comparison of Ultrasonic and Optical Images of Tonsil Using Perfluorocarbon Contrast and Horseradish Peroxidase Targeted to Epithelium with Anticytokeratin Antibodies

Peak Detected Image
100μm step size

Immunostained Tonsil

Figure 17. Peak Detected Ultrasonic Radiofrequency Images of Tonsil Epithelium Acoustically Enhanced with Anticytokeratin Antibody Targeted Perfluorocarbon Emulsion

Peak Detected Image
100μ Step Size

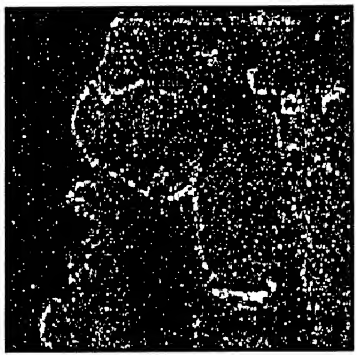

Zoom: 50μ step size

FIG. 18

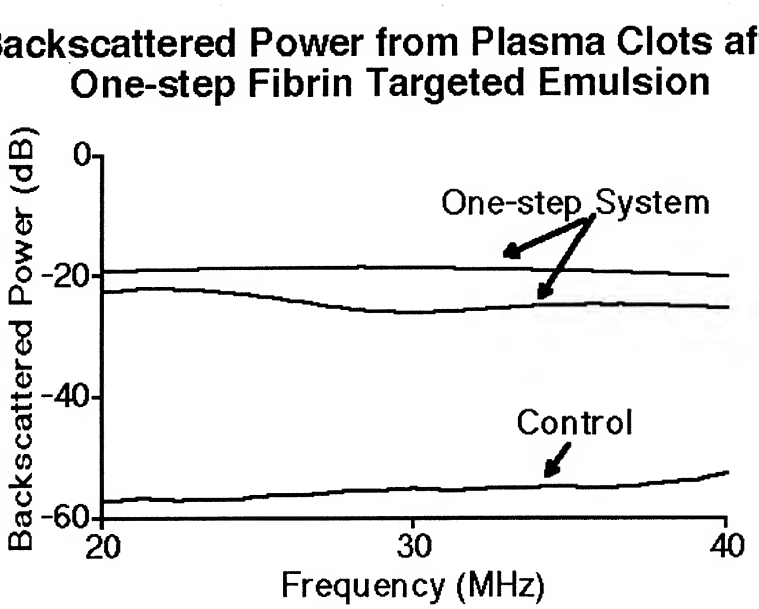
Backscattered Power from Plasma Clots after One-step Fibrin Targeted Emulsion
Backscattered Power (dB)
0
-20
-40
-60
One-step System
Control
20
30
40
Frequency (MHz)

FIG. 19

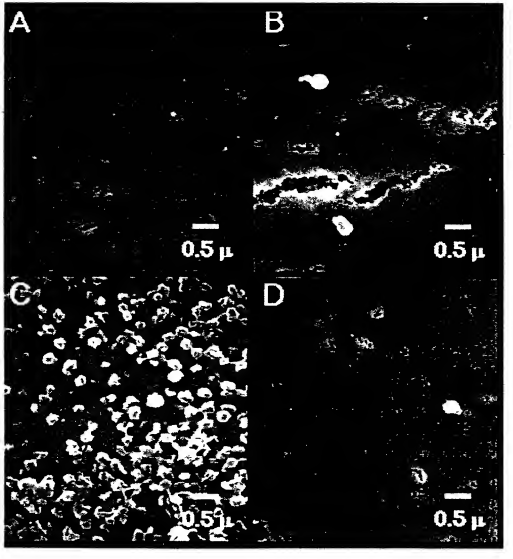

FIG. 20

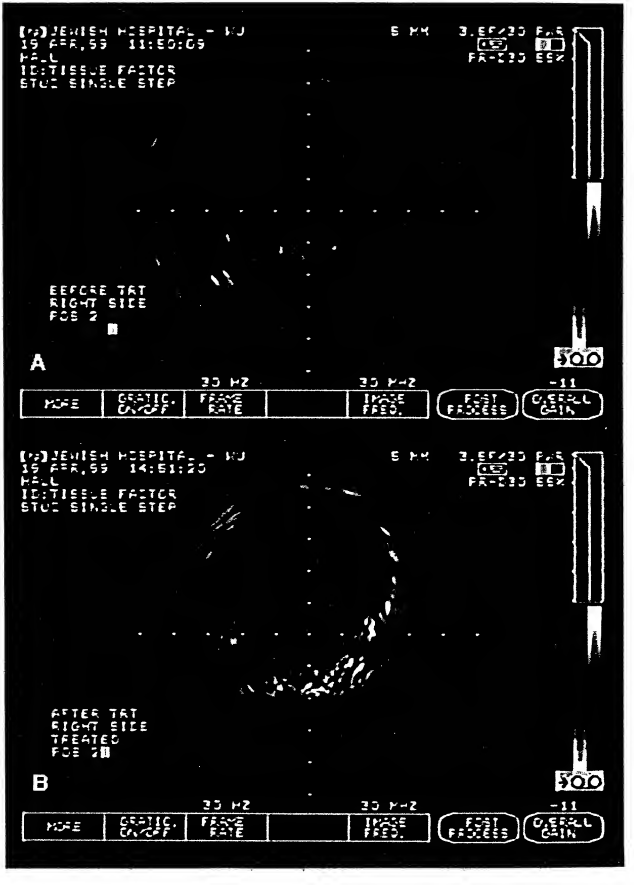
BEFORE TAT
RIGHT SIDE
FOR 2
A
30 MZ
30 MHZ
-11
MORE
GRAYSC. ON/OFF
IMAGE RATE
IMAGE FREQ.
POST PROCESS
OVERALL GAIN
AFTER TAT
RIGHT SIDE
TREATED
FOR 20
B
30 MZ
30 MHZ
-11
MORE
GRAYSC. ON/OFF
IMAGE RATE
IMAGE FREQ.
POST PROCESS
OVERALL GAIN

FIG. 21